PAPER

Check for updates

Green hydrogen and platform chemicals production from acidogenic conversion of brewery spent grains co-fermented with cheese whey wastewater: adding value to acidogenic CO_2

Omprakash Sarkar, Ulrika Rova, Paul Christakopoulos and Leonidas Matsakas [ID] *

The biotechnological production of fuel and chemicals from renewable, organic carbon-rich substrates offers a sustainable way to meet the increasing demand for energy. This study aimed to generate platform chemicals, which serve as precursors for the synthesis of fuels and various materials, along with green hydrogen (bio-H_2) by co-fermenting two different waste streams: brewery spent grains and cheese whey (CW). Reactors fermenting a fixed quantity of brewery-spent grains were loaded with CW at 20, 30, and 40 g COD per L, and microbial production of short-chain (SCCA) and medium-chain carboxylic acids (MCCA) along with bioH$_2$ was assessed. The reactor with the highest organic load (40 g COD per L) produced the highest amount of SCCA (21.67 g L^{-1}) whereas bio-H_2 was with 30 g COD per L (181.35 mL per day). In the next phase, the generated gas (H_2 + CO_2) was continuously recirculated within the reactor to enhance SCCA production by a further 19.9%. In the later stages of fermentation, MCCA production indicated the occurrence of chain elongation from the accumulated lactic acid. Consumption of H_2 and CO_2 during gas recirculation highlighted the role of bio-H_2 as an electron donor and acidogenic CO_2 as a precursor molecule in the chain elongation process. As a result, no external reducing agent was required and only limited CO_2 was released in the atmosphere, making the overall process more sustainable and cost-effective.

Introduction

Fossil-based fuels in the form of coal, oil, and natural gas remain the source of 80% of the world's energy, but they also strongly contribute to global warming.[1] Burning fossil-based fuels accounts for 89% of human-derived CO_2 emissions and, according to the Intergovernmental Panel on Climate Change, could cause global mean surface temperatures to rise by 1.5 °C above the pre-industrial mark in as little as a decade. To prevent catastrophic warming, it will be necessary to replace these fossil-based fuels with a sustainable alternative for energy and material synthesis.[2] Hydrogen is considered one of the most promising energy carriers due to its elevated energy density (141.9 MJ kg^{-1}), clean emissions (H_2O as the only combustible byproduct), and widespread abundance.[1,3–5] Recently, the hydrogen has been pitted as a significant upcoming energy source in our global landscape and thus both develop and developing nations and are making the low carbon energy source a central part of their strategy to decarbonize.

Currently H_2 production *via* electrolysis of water, steam reforming of natural gas followed by cracking oil products, coal gasification remains the main route, whereas less energy-demanding biological processes for hydrogen production are considered a promising alternative, which have garnered increasing attention.[6] Dark fermentation/acidogenic fermentation is a versatile process capable of efficiently converting various organic substrates (waste/wastewater) to bio-hydrogen (bio-H_2) under ambient temperature and pressure.[3,6–8] The added advantage of acidogenic fermentation is co-production of short-chain carboxylic acids (SCCA), including acetic (C2), propionic (C3), butyric (C4), and valeric (C5) acids, which can serve as platform chemicals for industrial applications.[9,10] The demand for volatile fatty acids (VFAs), including the above SCCA, is expected to increase over the coming years due to their numerous applications as fuel precursors, as well as in pharmaceutical, and household chemical formulations.[2,11] While global production of chemicals doubled over the past two decades, reaching 2.3 billion tons in 2017, only 2% of them were bio-based. Furthermore, fossil-based chemical production consumes 20% of the energy used for industrial purposes. Switching from a fossil-based to a bio-based economy remains a challenge, but it represents also a necessary step to meet the UN Sustainable Development Goals.
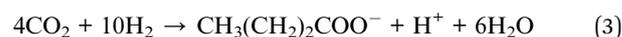
Biochemical Process Engineering, Division of Chemical Engineering, Department of Civil, Environmental, and Natural Resources Engineering, Luleå University of Technology, 971-87 Luleå, Sweden. E-mail: leonidas.matsakas@ltu.se; Tel: +46 920 493043

Importantly, SCCA can be upgraded to value-added caproic acid (C6) and other medium-chain carboxylic acids (MCCA) *via* reverse β-oxidation in the presence of an external electron donor, such as ethanol, methanol or lactic acid.[11–15] During reverse β-oxidation, SCCA are elongated *via* the addition of two carbon atoms per cycle,[16–19] while the electron donor is converted to acetyl-CoA, acetoacetyl-CoA, and butyryl-CoA. The latter can react with acetate to generate butyrate, while another acetyl-CoA can react with butyryl-CoA to form caproyl-CoA, and thereby lead to caproate.[19,20] The conversion of SCCA to MCCA is carried out by microorganisms and a crucial role is played by electron donors.[21,22] Increasing attention has been garnered by new solutions such a carboxylate platform with mixed culture fermentation for the production of MCCA (6 to 12 carbon atoms) through carboxylic chain elongation.[18] With high caloric value and slightly hydrophobic properties, caproic acid is a suitable intermediate for biofuel (*i.e.*, isobutyl hexanoate as drop-in additive in A-1 jet fuel), pharmaceuticals,[18] and biochemical production.[23] Moreover, upgrading SCCA to MCCA *via* reverse β-oxidation can help overcome the limitations associated with the high costs of recovery and purification of SCCA.[24] Moreover, MCCA have a higher market value than SCCA, estimated at 2000–3000 $ per t, and a market demand of 25 000 tons per year.

The aim of this study was to evaluate the production of acidogenic bio-H$_2$ and carboxylic acids from a renewable feedstock such as brewery-spent grains (BSG) co-fermented with cheese whey (CW). These two waste streams complement each other, as BSG is rich in protein and polysaccharides, while CW is rich in lactose. Co-fermentation enhances system stability and the synthesis of microbial metabolites due to synergistic effects that promote a more diverse microbial community, better nutrient balance, and access to trace elements essential for the fermentation process.[25] For a large-scale application, fermentation of this waste/wastewater can be conjugated with the existing anaerobic digestion/sewage treatment plants modifying the input parameters (such as pH, nature of biocatalyst and substrate load) in a bio-refinery approach to have greatest impact to produce platform chemicals and bio-hydrogen. The study was conducted in two phases. Phase-I (P-I) focused on the effect of varying the organic load of CW on SCCA and MCCA generation, using as electron donor the lactic acid produced during mixed culture fermentation. Phase-II (P-II) followed the same layout as P-I, except that it aimed at enhancing production of both SCCA and MCCA through recirculation of the biogas released during acidogenic fermentation. This is due to the composition of the acidogenic biogas being 40–50% H$_2$ and 50–60% CO$_2$, in which the cogenerated CO$_2$ limits the use of bio-H$_2$ as a fuel. Many studies have demonstrated the utilization/removal of acidogenic CO$_2$ by adopting different strategies such as chemical/physical adsorption, membrane/vacuum separation, electrochemical processes *etc*[26]. Despite these processes significantly upgrades the bio-H$_2$, poses a few limitations to these processes as the captured CO$_2$ is released back into the atmosphere and amplifies greenhouse heating. CO$_2$ storage and capturing technologies on the other hand are expensive, at the same time developing a process towards sequestration of CO$_2$ for the sustainable production of fuels and chemicals become a current research hotspot and has important strategic and real economic significance.[27–29] Currently numerous studies has been carried out finding a potential mitigation options such as utilization of low carbon dependent fuels as chemicals/feedstock's and fuels including biomass as well as CO$_2$ capture and storage (CCS) in order to reduce greenhouse gas (GHG) emissions.[30] Moreover, the separation processes for CO$_2$ demands retrofitting to the traditional processes, which directly influence the overall investment. On the other side, the biological routes offers an attractive approach for the utilization/conversion of CO$_2$ as the operating principle towards CO$_2$ reactions occurs naturally occur in microbes (eqn (1)–(3)).[31–33]

$$2CO_2 + 4H_2 \rightarrow CH_3COO^- + H^+ + 2H_2O \quad (1)$$

$$2CH_3COO^- + H^+ + 2H_2 \rightarrow 2CH_3(CH_2)_2COO^- + 2H_2O \quad (2)$$

$$4CO_2 + 10H_2 \rightarrow CH_3(CH_2)_2COO^- + H^+ + 6H_2O \quad (3)$$

"CO$_2$-reducing acetogen" or a "homoacetogen" takes acetyl-CoA biochemical pathway for the formation of acetic acid as fermentation product from CO$_2$.[33,34] Thus, here we studied the utilization of the *in situ* CO$_2$ produced during acidogenic co-fermentation of cheese whey and BSG for an enhanced biosynthesis of microbial metabolites, at the same time to limit the release of CO$_2$ into the environment.

Experimental

Inoculum

Anaerobic sludge was collected from a biogas plant in Luleå, Sweden. The sludge was filtered using a stainless steel mesh to remove grit and other solid particles (*e.g.*, hair and paper) and allowed to settle overnight. The supernatant (mostly water) was removed and the thickened sludge with a volatile solids (VS) content of 0.56 g g^{-1} was used as biocatalyst. Prior to use, 2-bromoethanesulfonic acid (4 g L^{-1}) was added to the sludge to suppress methanogens. To promote an active bacterial population, the sludge was incubated at ambient temperature for 72 h with a nutrient solution containing 5 g L^{-1} glucose, 0.5 g L^{-1} NH$_4$Cl, 0.25 g L^{-1} KH$_2$PO$_4$, 0.25 g L^{-1} K$_2$HPO$_4$, 0.3 g L^{-1} MgCl$_2$, 25 mg L^{-1} CoCl$_2$, 11.5 mg L^{-1} ZnCl$_2$, 10.5 mg L^{-1} CuCl$_2$, 5 mg L^{-1} CaCl$_2$, 15 mg L^{-1} MnCl$_2$, 16 mg L^{-1} NiSO$_4$, and 25 mg L^{-1} FeCl$_3$, before inoculation in the reactor system.

Feedstock preparation and characterisation

BSG used in this study was provided by Skellefteå Bryggeri (Skellefteå, Sweden). Prior to use, BSG was oven-dried at 65 °C for 12 h and stored in a sealed bag. Highly heterogeneous BSG was homogenised using a kitchen mixer (SM-1FP; Wilfa), which delivered particles of 0.5–1 cm. The homogenised BSG contained 96.2% ± 0.02% w/w total solids, of which 94.2% ± 0.03% w/w were VS. Cellulose, hemicellulose, and lignin accounted for 29.35%, 16.64%, and 13.33% w/w of BSG, respectively. CW was provided by Norrmejerier, Sweden. Prior to use as substrate, the

Table 1 Acidogenic conversion of brewery-spent grains (BSG) co-fermented with a varied organic load of cheese whey wastewater (CW) in phases

Experiment	BSG load (g VS)	CW load (g COD per L)	Fermentation time (days)
Phase-I			
R_{20}	35	20	56
R_{30}	35	30	56
R_{40}	35	40	56
Phase-II (gas recirculation)			
$GC-R_{20}$	35	20	56
$GC-R_{30}$	35	30	56
$GC-R_{40}$	35	40	56

organic content of CW was determined as 75.6 g chemical oxygen demand (COD) per L while pH was 5.7. A major fraction of CW was represented by lactose (48 g L^{-1}), along with traces of lactic acid (0.04 g L^{-1}), acetic acid (0.08 g L^{-1}), propionic acid (0.01 g L^{-1}), and butyric acid (0.07 g L^{-1}). Based on the required organic load (20, 30, and 40 g COD per L), CW was diluted with tap water.

Experimental procedure

The experiments were conducted in 18 identical 2000 mL glass bottle reactors (triplicates of six experiments) in two phases (P-I and P-II) using the AMPTS-II automated analytic system (Bioprocess Control). During P-I, the effect of varying the organic load of CW on carboxylic acids and bio-H_2 recovery was

evaluated. The biogas ($H_2 + CO_2$) produced during acidogenic fermentation was recirculated in P-II to provide a source of inorganic carbon (CO_2) and an electron donor (H_2) for the homoacetogens in the mixed culture. Based on the experimental design and conditions, reactors were labelled as R_{20} (20 g COD per L), R_{30} (30 g COD per L), and R_{40} (40 g COD per L) when operated in P-I, and GC-R_{20} (20 g COD per L), GC-R_{30} (30 g COD per L), and GC-R_{40} (40 g COD per L) in P-II, with GC corresponding to gas recirculation (Table 1 and Fig. 1). All reactors were operated for 56 days in batch mode under mesophilic conditions (35 °C). No further nutrients were added during fermentation because BSG was sufficiently rich. Prior to start up, the pH in the reactors was adjusted using 2 M HCl/NaOH, after which it was set manually to 6.0–6.5. Nitrogen gas was sparged into the reactor for 30 min to maintain anaerobic conditions. The reactors were kept in suspension mode during the reaction phase by continuous mixing with a stirrer fixed to the cap. All fermentation tests and measurements were conducted in triplicate, and the average values and standard deviation were reported.

Biochemical and gas analyses

COD of CW was analyzed using the Spectroquant NOVA 60A COD cell test kit (Merck Millipore). Changes in pH were measured with a pH meter (pHenomenal-pH1100L; VWR). Total solids (TS) and volatile solids (VS) were estimated as described by Matsakas *et al.* (2020).[35] Microbial metabolites, including lactic (H_{Lac}), acetic (H_{Ac}), propionic (H_{Pr}), butyric (H_{Bu}), valeric (H_{Val}), and caproic (H_{Ca}) acids, were analysed by high-performance liquid chromatography (HPLC) and quantified with calibration curves generated
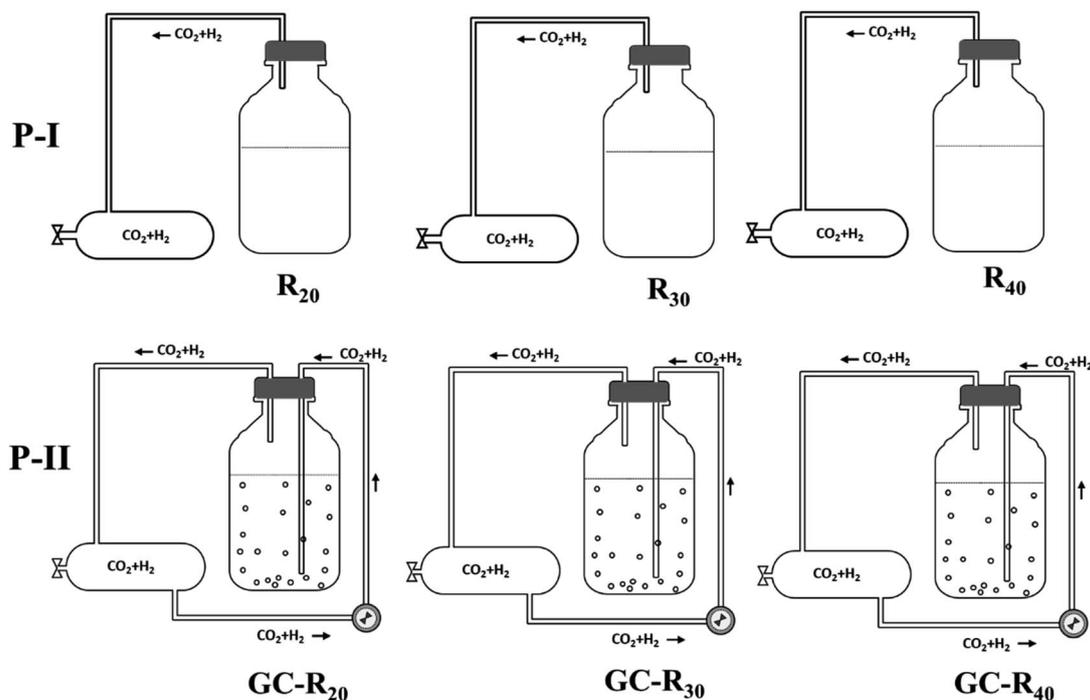

Fig. 1 Overlay of the experimental designed which was conducted in two phases (P-I & P-II). Initially an influence of varied organic load of CW (20, 30 and 40 g COD per L) as co-fermenting substrate with BSG (35 g VS) on microbial metabolites was studied in P-I. P-II was similar as P-I, additionally here the produced biogas was recirculated in the reactor evaluating its influence on microbial metabolites.

from commercially available standards (10 mM, Volatile Free Acid Mix; Sigma). The HPLC apparatus (PerkinElmer) was equipped with a Flexar LC pump, Bio-Rad Aminex HPX-87H column (300 m × 7.8 mm), and PerkinElmer-200 refractive index detector. Column temperature was maintained at 65 °C. The mobile phase consisted of 5 mM H_2SO_4 and was eluted at 0.6 mL min^{-1}. Biogas production and composition was analyzed using a mass spectrometer (GAM 400; InProcess Instrument).

Results and discussion

Total carboxylic acids production

Co-fermentation of protein and carbohydrate-rich BSG and CW enhanced carboxylic acid production beyond what had been observed previously when using BSG as sole carbon source.[36] Production performance was investigated by varying the COD of CW (20, 30, and 40 g COD per L) while maintaining a fixed BSG content (35 g VS). Total carboxylic acid production increased with fermentation time in all reactors (Fig. 2), with variations based on the initial COD. Specifically, production was more or less similar until day 8, when it ranged around 3.45–4.66 g L^{-1}, and increasing to 9.47–10.06 g L^{-1} by day 16 (Fig. 2a). On day 24, the three reactors displayed diverging patterns, with R_{40} attaining a production of 19.63 g L^{-1}, followed by R_{30} (12.89 g L^{-1}) and R_{20} (11.58 g L^{-1}). By day 40, reactor R_{40} reached 24.53 g L^{-1}, while R_{30} followed with 22.06 g L^{-1} and R_{20} with 13.21 g L^{-1}. By the end of the experiment (day 56), reactor R_{30} decreased slightly to 20.91 g L^{-1}, whereas R_{40} gradually increased production to 26.35 g L^{-1} and R_{20} to 16.14 g L^{-1}. Overall, reactor R_{40} achieved 1.6-times and 1.2-times greater production than R_{30} and R_{20}, respectively.

Previously Teixeira et al., found a good carboxylic acids production of 43.8 g COD as a major microbial metabolites from an untreated BSG during a long-term (HRT 41 days) fed-batch acidogenic fermentation.[37] Liang and Wan demonstrated a mixture of carboxylic production from BSG at alkaline pH 10 with higher fraction of acetic acid (6.3 g L^{-1}).[38] In a two-step conversion of acid pretreated hydrolysate of BSG, Guarda et al. (2021) found a mixture of carboxylic acids (9 ± 1.59 g COD per L) from a continuously operated reactor at an organic load rate (OLR) of 8.11 ± 0.87 g COD per L per day.[39] Fermenting the hydrolysate derived from BSG through acid pretreatment, Mussatto et al. (2007) showed a lactic acid production of 5.4 g L^{-1} by *Lactobacillus delbrueckii*.[40]

Composition of carboxylic acids (P-I)

Total carboxylic acids included H_{Lac}, H_{Ac}, H_{Pr}, H_{Bu}, H_{Val}, and H_{Ca}. Their individual concentration varied with respect to fermentation time, VS, and COD load (Fig. 3). The reactor with the highest COD achieved also the highest H_{Lac} output (Fig. 3a). The concentration of H_{Lac} was maximal between 8 and 24 days, with peak production of 9.7 g L^{-1} (10.38 g COD per L, R_{40}; day 24), followed by 6.8 g L^{-1} (R_{30}; day 24) and 3.6 g L^{-1} (R_{20}; day 16). These amounts corresponded to 41.12%, 37.6%, and 31% of the total carboxylic acids accumulated in the reactor, and reflected the influence of a higher COD, and hence lactose content, in CW. Mixed culture fermentation converts monosaccharides and disaccharides to H_{Lac}.[41] Lactose-rich CW is initially broken down to glucose and galactose, after which it is converted to H_{Lac} via the glycolytic pathway.[23,42] Similarly,
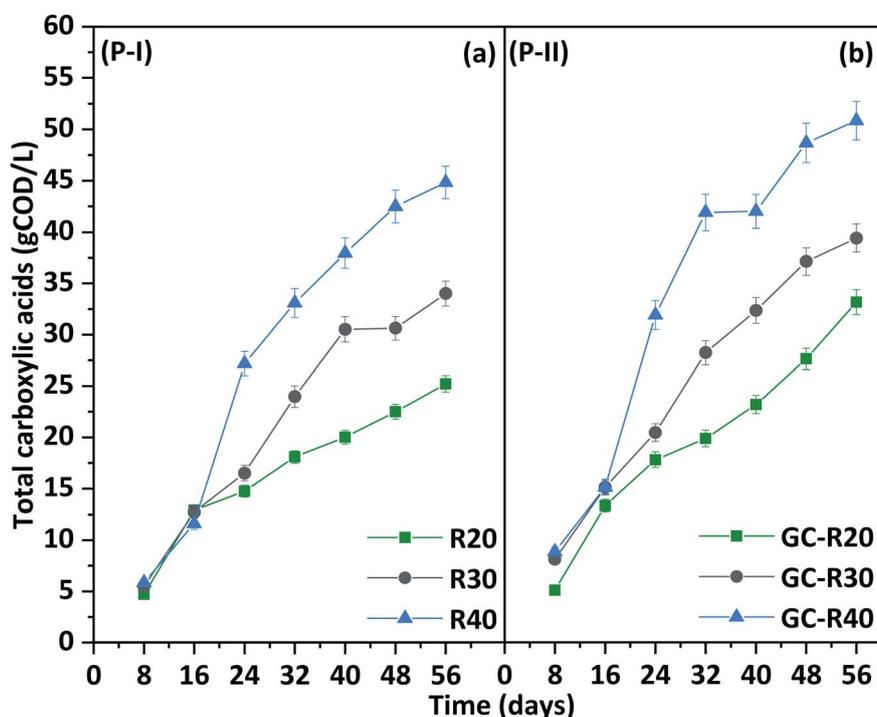

Fig. 2 Total carboxylic acids production from a fixed quantity of BSG (35 g VS) co-fermented with a varied organic load of CW (20, 30 and 40 g COD per L) in phase-I (P-I) and phase-II (P-II) where the acidogenic CO_2 was recirculated within the reactor in phase-II.
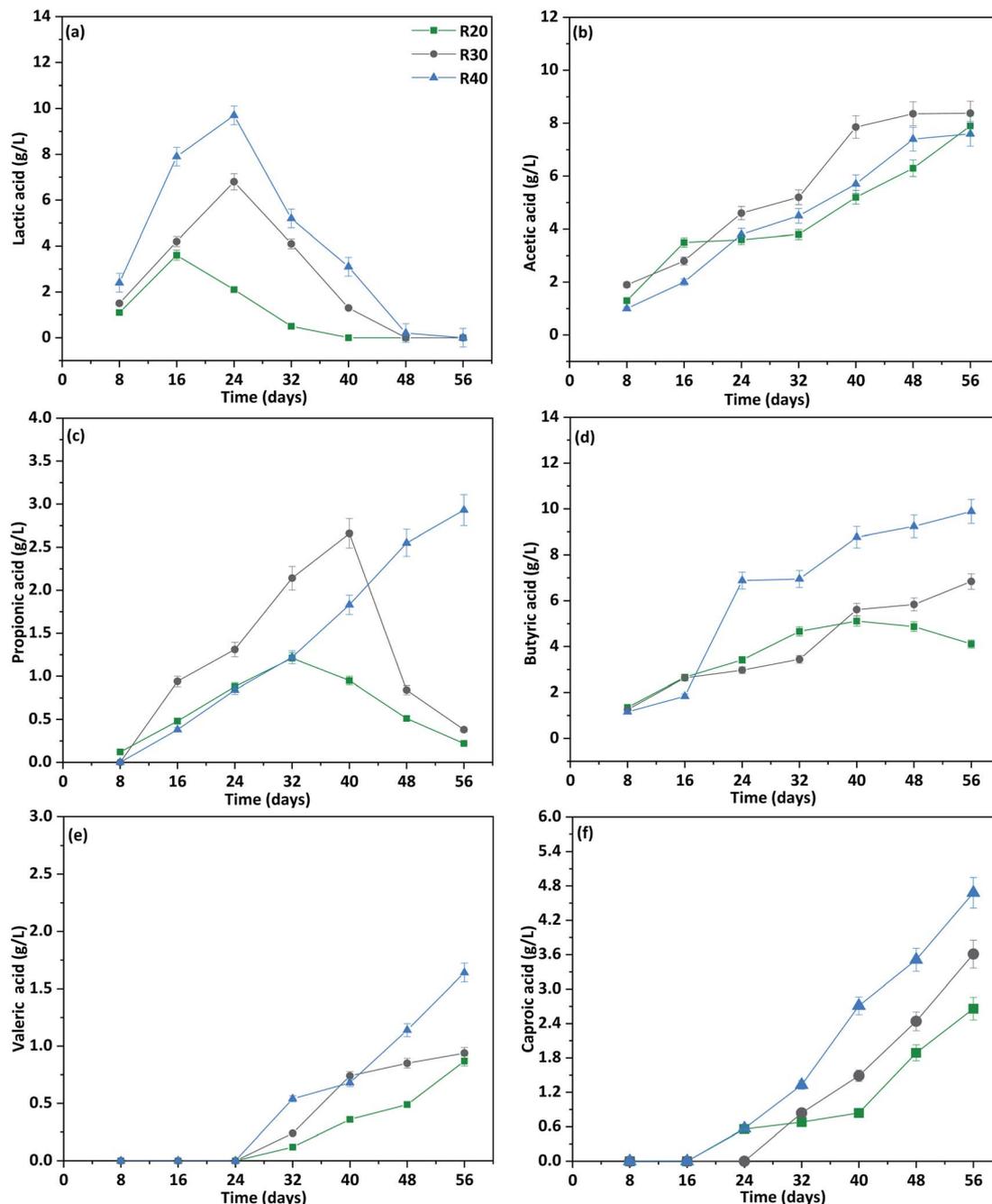
Fig. 3 Composition of carboxylic acids (a–f) derived from co-fermentation of BSG and different organic load of cheese whey with respective to fermentation time in phase-I (P-I).

pyruvate can be converted through acetyl-CoA to ethanol, H_{Ac}, H_{Bu} or even other metabolites depending on the microbial microenvironment.[23] Yu *et al.* (2004) detected a mixture of carboxylic acids and solvents during acidogenic fermentation of lactose-rich wastewater at pH 5.5.[43] Fermenting the high strength CW in a anaerobic sequencing batch reactor, Costa *et al.*, reported carboxylic acids production of 10.23 g COD per L accounting for 4.54 g COD per L per day,[44] Atasoy *et al.*, reported the production of 0.97 g COD per g SCOD with major fraction of butyric acid at alkaline condition in the batch reactor.[45]

H_{Ac} and H_{Bu} were the two major carboxylic acid fractions, and their concentration gradually increased with fermentation time; whereas H_{Pr} remained low throughout the experiment (Fig. 3b–d). H_{Ac} biosynthesis was greater in reactor R_{30} (8.38 g L^{-1}), followed closely by R_{20} (7.9 g L^{-1}) and R_{40} (7.6 g L^{-1}) (Fig. 3b). In contrast, total H_{Bu} production was significantly higher (9.89 g L^{-1}) under high COD load in CW (R_{40}) compared to R_{30} (6.84 g L^{-1}) and R_{20} (5.11 g L^{-1}) (Fig. 3d). H_{Bu} biosynthesis occurs *via* (i) phosphotransbutyrylase and butyrate kinase, or (ii) butyryl CoA:acetate CoA transferase metabolic

pathways. Some members of *Clostridium* are capable of elongating H_{Lac} to H_{Bu} without the involvement of H_{Ca}, as they can convert butyryl-CoA to H_{Bu} through phosphorylation instead of *via* cyclical reverse β-oxidation.[20] Biosynthesis and concentration of H_{Pr} were relatively low compared to those of other carboxylic acids and were detected only after day 16 (Fig. 3c). In the present set-up, H_{Pr} production can be attributed to the degradation of proteins and carbohydrates present in BSG and CW through amino acid catabolic and biosynthetic pathways.[46] The stronger production of H_{Pr} in reactor R_{40} (2.25 g L^{-1}; day 48) compared to R_{30} (1.53 g L^{-1}; day 40) and R_{20} (1.2 g L^{-1}; day 40) is related to a greater availability of amino acids. A decline in H_{Pr} was noticed by the end of the experiment, indicating its biotransformation, together with H_{Ac} and H_{Bu}, to H_{Val} and H_{Ca}. An increasing concentration of these carboxylic acids in the reactor, along with their simultaneous transformation to longer-chain molecules during fermentation indicated an efficient and continuous hydrolysis of BSG by a mixed microbial culture, which delivered a continuous stream of sugars for fermentation.

Unlike other carboxylic acids, H_{Val} and H_{Ca} were not detected during the initial stages of fermentation (Fig. 3e and f). H_{Val} production started on day 32 with relatively low levels (0.54 g L^{-1} for R_{40}; 0.24 g L^{-1} for R_{30}, and 0.12 g L^{-1} for R_{20}) (Fig. 3e). These values gradually increased with time and reached a maximum on day 56, with 1.64 g L^{-1} in R_{40}, 0.94 g L^{-1} in R_{30}, and 0.87 g L^{-1} in R_{20}.

Production and consumption rate of carboxylic acids (P-I)

The production (P_{rate}) and consumption rate (C_{rate}) of carboxylic acids showed a distinct trend with respect to the initial load of CW in the reactor and fermentation time (Fig. 4). In P-I, P_{rate} of H_{Bu} was significantly higher compared to other carboxylic acids. Initially until day 16, the P_{rate} of H_{Bu} was ranged between 0.08–0.31 g COD per L per day in all the reactors which later increased on day 24 specifically with R_{40} exhibiting the highest P_{rate} of 1.15 g COD per L per day. Further from day 48, its consumption was observed with R_{20} (−0.05 g COD per L per day) which later increased to −0.17 g COD per L per day during day 56 and stabilized thereafter. H_{Bu} consumption was not seen with R_{30} and R_{40} indication its acidogenic production and continuous accumulation in the reactor with a P_{rate} of 0.11–0.23 g COD per L per day despite its transformation to chain elongated H_{Ca}. P_{rate} of H_{Ac} was maximum with R_{30} (0.36 g COD per L per day) followed by R_{20} (0.29 g COD per L per day) and R_{40} (0.24 g COD per L per day) on different time interval of fermentation. H_{Pr} production was started after day 8, by day 16, P_{rate} of H_{Pr} reached to 0.15 g COD per L per day (R_{30}), however its maximum P_{rate} was noticed on day 40 with R_{40} (0.17 g COD per L per day). Afterwards its consumption from day 48, particularly with R_{20} and R_{30} reduced its concentration to less than 0.91 g COD per L and 1.72 g COD per L respectively. On the contrary, although the production declined (P_{rate} of 0.02 g COD per L per day), its consumption was not documented until the end of the cycle, indicating its continuous biosynthesis from the fermentable sugars by mixed culture. Initially with a P_{rate} ranging between 0.03 to 0.14 g COD per L per day, H_{Val} production was noticed from day 32. Later its P_{rate} slightly decreased on day 48 (0.03–0.12 g COD per L per day), later no great improvement was observed indicating a stabilized production.
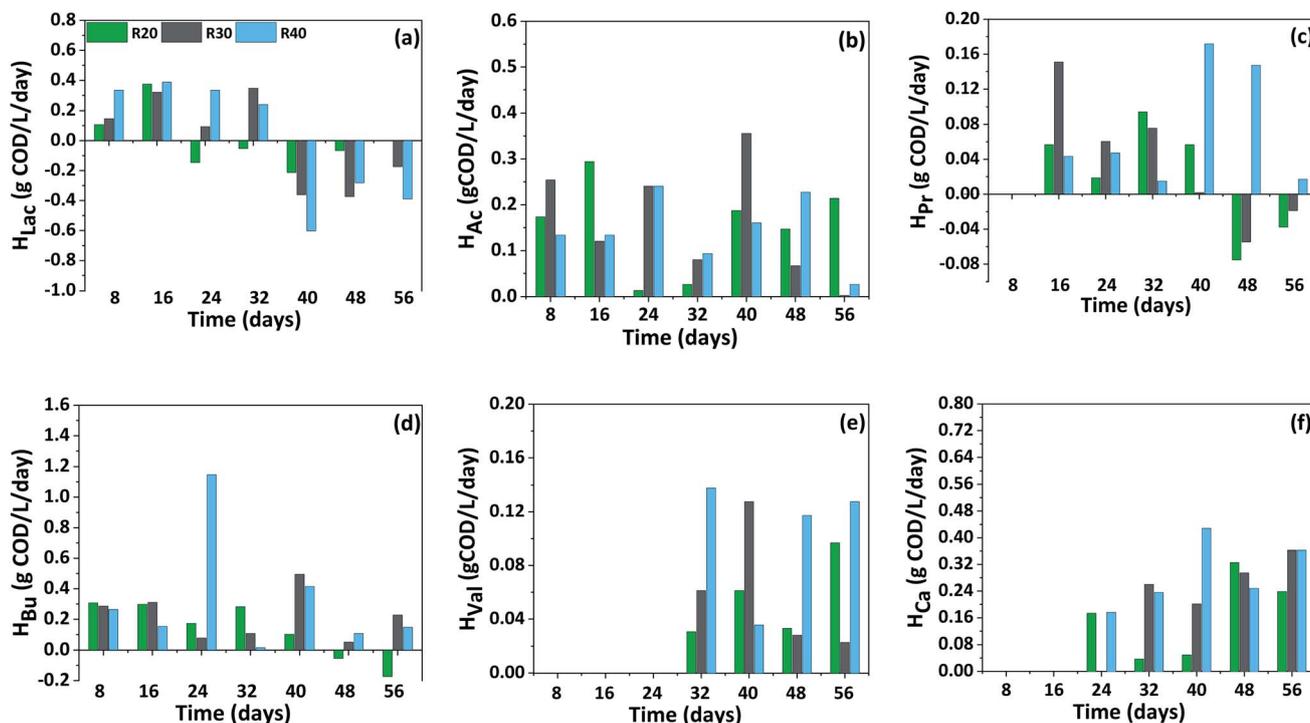

Fig. 4 Distribution of carboxylic acids production (P_{rate}) and consumption rate (C_{rate}) pattern in P-I (a–f) with respect to fermentation time.

Biogas production (P-I)

At the end of the experiment (day 56), the composition of the gas in the bags being connected to the headspace of the reactors was analysed. The highest total biogas level was recorded with reactor R_{30} (16.13 L), followed by R_{40} (15.30 L) and R_{20} (14.98 L) (Fig. 5). Most gas (>90%) was produced between 8 and 16 days, thereafter, biogas production declined. Composition analysis of the total biogas revealed that the overall volumetric bio-H_2 production amounted to >8 L in all reactors, with the highest accumulation in reactor R_{20} (67%; day 4), followed by R_{30} (62%; day 8) and R_{40} (55%; day 8). The highest cumulative bio-H_2 production was recorded with R_{30} (9.31 L), followed by R_{20} (9.25 L) and R_{40} (8 L) Fig. 5b). The comparatively lower production of bio-H_2 at a higher COD might be due to an overload of organic substrate in the system, which slowed down microbial metabolism, as lactose-rich CW could not be metabolised by all microbes. Assessment of the production profile with respect to fermentation time revealed that the largest volume of bio-H_2 was generated within 16 days (>95%), declining thereafter. Specifically, reactors R_{40}, R_{20}, and R_{30} accounted for 83%, 82%, and 79.61% of total volumetric bio-H_2 production, respectively. Bio-H_2 is generated preferentially during short retention times due to the rapid accumulation of microbial metabolites (mostly carboxylic acids) *via* acidogenesis. Despite low microbial metabolism after day 12, the reactors were operated for 56 days to further enhance conversion of substrate to carboxylic acids.

Bio-H_2 production depends on several operating conditions, such as substrate type/concentration, redox microenvironment, and nature of inoculum. Indeed, a pH of 5.7–6.0 favours acidogenic fermentation and, consequently, both bio-H_2 release and chain elongation. Even though the generation of bio-H_2 was much lower from day 13 to 28, it nevertheless amounted to almost 1.89 L (R_{30}), 1.62 L (R_{20}), and 1.33 L (R_{40}) (). As shown here one of the best ways to positively exploit the carbohydrate and protein content of CW and BSG as waste feedstocks, is through generation of bio-H_2 and soluble metabolites, such as SCCA and MCCA.[36,47,48] When looked into the yields from its initial load of carbohydrate in the reactor, the highest value was found with R_{20} (216.46 mL H_2/$g_{carbohydrate}$) followed by R_{30} (194.66 mL H_2/$g_{carbohydrate}$) and R_{40} (146.70 mL H_2/$g_{carbohydrate}$). BSG co-fermented with CW was found to be an ideal feedstock for acidogenic bio-H_2 production due to its high organic load in the form of soluble carbohydrates.[49,50]
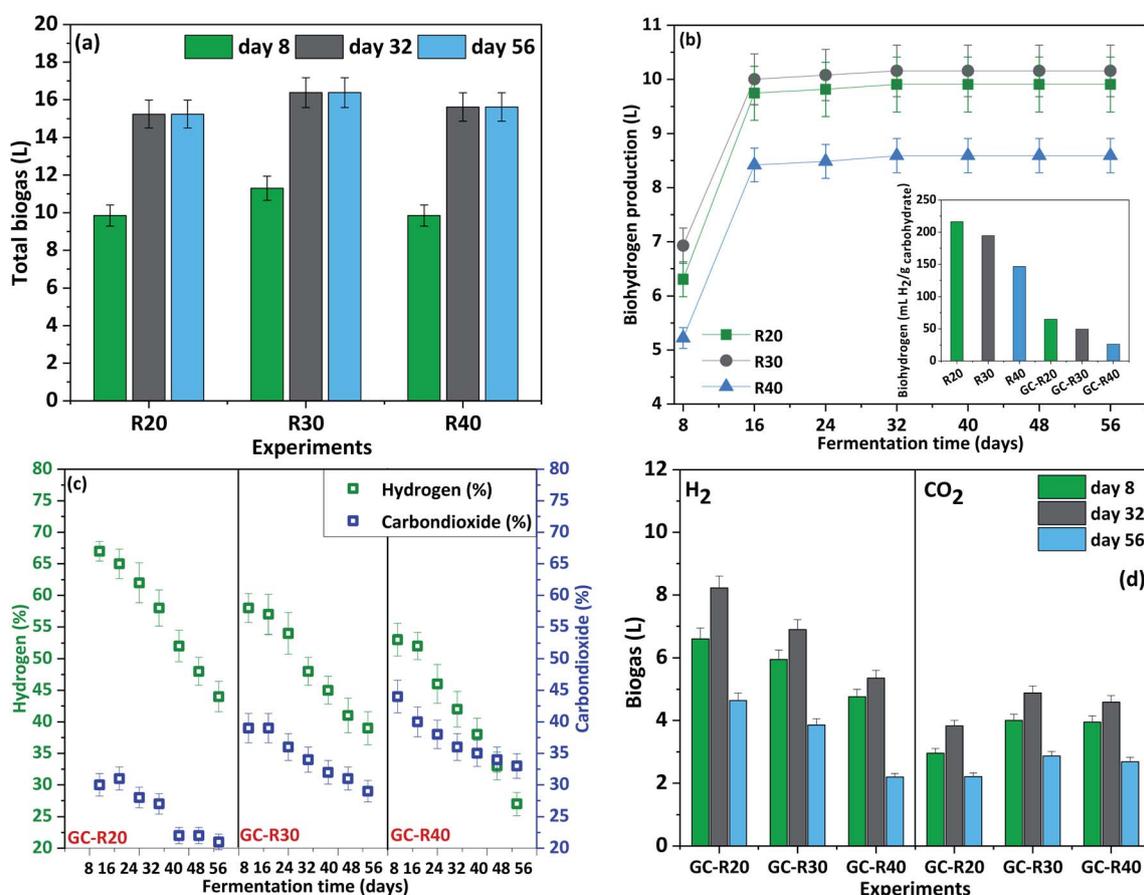
Fig. 5 (a) Total biogas production during acidogenic co-fermentation of BSG and CW at organic load of 20, 30 & 40 g COD per L in P-I, (b) volumetric biohydrogen production measured in the total biogas of P-I, biohydrogen yield (figure as inset) (c) production and consumption of acidogenic H_2 and CO_2 during biogas recirculation within the reactor in P-II, (d) volumetric production and consumption of biogas in the reactor during its recirculation in P-II.

Biogas production (gas recirculation: P-II)

Along with carboxylic acids, acidogenic fermentation cogenerates CO_2 and H_2. In particular, almost 30% of the substrate is broken down to CO_2, this impacts carboxylic acid production during fermentation.[51] The reutilisation of this CO_2 could benefit the production of carboxylic acids. In this study, the biogas released during acidogenic fermentation was recirculated continuously at a flow rate of 80 mL h^{-1}. Gas consumption and composition were analysed periodically. Up until day 16, bio-H_2 content was 65–67% (GC-R_{20}), 57–58% (GC-R_{30}), and 52–53% (GC-R_{40}), corresponding to a volumetric bio-H_2 accumulation of 9.26 L, 9.05 L, and 7.90 L, respectively; whereas CO_2 accounted for 30–31% (GC-R_{20}), 38–39% (GC-R_{30}), and 40–44% (GC-R_{40}) of generated biogas (Fig. 5c). Consumption of both bio-H_2 and CO_2 was observed after day 16 in all reactors and, by day 24, the proportion of bio-H_2 declined slightly to 62% (GC-R_{20}), 54% (GC-R_{30}), and 46% (GC-R_{40}). After day 32, both bio-H_2 and CO_2 exhibited a significant decline. Eventually, by day 56, bio-H_2 content was only 44% (GC-R_{20}), 39% (GC-R_{30}), and 27% (GC-R_{40}); while CO_2 amounted to 21% (GC-R_{20}), 29% (GC-R_{30}), and 33% (GC-R_{40}) of biogas. These values indicated significant consumption of H_2 and CO_2 during recirculation in the reactor.

The availability of H_2 and CO_2 in the reactor favours homoacetogens, which can grow both autotrophically on H_2 and CO_2 and/or heterotrophically through consumption of organic compounds. Previously Luo et al., (2011) observed a consumption of 11–43% of H_2 by homoacetogens grown on a single carbon source in batch fermentations.[52] Moreover, CO_2 acts as the terminal electron acceptor as well as carbon source for homoacetogens. Arslan et al. (2012) reported increased carboxylic acids production by a mixed culture when the reactor headspace was supplemented with H_2 and CO_2 at a pressure of 2 bar.[53] CO_2 released during fermentation is consumed again and converted to acetic acid during acetogenic fermentation. Because 5% to 10% of the reducing equivalents required for fixing the evolved CO_2 are used to sustain microbial growth, complete CO_2 recycling is not energetically possible without external energy supplementation. During recirculation, bio-H_2 serves as electron donor to provide the energy required for biomass production and cell maintenance and, therefore, does not impose a loss of carbon in acetogens. Upon consumption, the yields observed here by the end of the experiment from the initial load of carbohydrate was 101.36 mL $H_2/g_{carbohydrate}$ followed by 73.90 mL $H_2/g_{carbohydrate}$ and 37.5 mL $H_2/g_{carbohydrate}$ with GC-R_{40}, GC-R_{40}, and GC-R_{40} respectively from its initial yield of 202.46 mL $H_2/g_{carbohydrate}$, 173.47 mL $H_2/g_{carbohydrate}$ and 135 mL $H_2/g_{carbohydrate}$ respectively noticed during initial phases (8–16 days) of fermentation. With recirculation, the H_2 and CO_2 in the total biogas was consumed gradually resulted with its decreased volume with time. By the end of the experiment (day 56), with consumption of 5.71 L and 3.4 L of H_2 and CO_2 respectively, GC-R_{40} was found to be more efficient suggesting its utilization towards formation of microbial metabolites. On the other side, its consumption with GC-R_{30} (5.19 L: H_2; 3.33 L: CO_2) and GC-R_{20} (4.63 L: H_2; 2.21 L: CO_2) was slightly less compared to GC-R_{40} (Fig. 5d). No CH_4 was detected throughout the process due to suppression of methanogens following addition of 2-bromoethanesulfonic acid.

Carboxylic acid production during gas recirculation (P-II): adding value to CO_2 from acidogenic fermentation

Biogas produced during fermentation was recirculated to evaluate the effect of H_2 and CO_2 on carboxylic acid production. This strategy significantly enhanced the output of carboxylic acids compared to P-I (Fig. 6). By the end of the cycle (day 56), the reactor with the lowest COD load in CW (GC-R_{20}) showed a 21% increment in SCCA + MCCA, followed by 12.29% (GC-R_{30}) and 11.75% (GC-R_{40}) (Fig. 2b). Compared to P-I, H_{Lac} biosynthesis was 9.55% (GC-R_{20}) higher in P-II on day 24, followed by 5.09% (GC-R_{40}) and 2.02% (GC-R_{30}) on day 32 (Fig. 6a). The accumulated H_{Lac} was completely consumed over time.

In case of H_{Ac}, production increased gradually almost from the start (day 4) in all reactors and displayed a significant increment compared to reactors operated in P-I (Fig. 6b). Specifically, an additional production of 2.47 g L^{-1} (GC-R_{40}), 1.38 g L^{-1} (GC-R_{30}), and 0.89 g L^{-1} (GC-R_{20}) in P-II meant that H_{Ac} reached a maximum of 9.87 g L^{-1}, 9.76 g L^{-1}, and 8.79 g L^{-1}, respectively, which was 25%, 14.1%, and 10.12% higher than in P-I. The enhanced H_{Ac} generated in this phase can be attributed to homoacetogens converting CO_2 to H_{Ac} in the presence of H_2 as electron donor,[33] confirming the impact of gas recirculation on homoacetogens enrichment. Gas recirculation had no major effect on H_{Pr}, which remained relatively low and showed a sustained increase only in reactor GC-R_{40} (Fig. 6c).

Chain elongation of H_{Ac} in the presence of an electron donor (H_2) led also to enhanced biosynthesis of H_{Bu} (Fig. 6d). H_{Bu} accumulation in P-II was higher with GC-R_{40} (11.22 g L^{-1}) compared to GC-R_{30} (7.46 g L^{-1}) or GC-R_{20} (6.86 g L^{-1}), resulting in 11.2%, 25.9%, and 40% greater H_{Bu} values with respect to P-I. The relatively lower H_{Bu} concentrations recorded with GC-R_{30} and GC-R_{40} over GC-R_{20}, despite their higher organic loads, might be explained by H_{Bu} chain elongation to other products. Gas recirculation potentially provides fermenting media with electron donors, which steer the direction and rate of fermentation towards specific products. Greater quantities of H_{Bu} formed in the reactors might accrue from two possible routes: (i) elongation of H_{Ac} to H_{Bu} utilising H_2, or (ii) direct reduction of CO_2 and H_2. Zhou et al. (2017) found a 68.2% increment in carboxylic acids production by sparging $H_2 : CO_2$ (80 : 20).[54]

H_{Val} biosynthesis was also favoured by gas recirculation (Fig. 6e). Indeed, H_{Val} production was anticipated from day 32 in P-I to day 24 in P-II, and was accompanied by an overall accumulation of 1.85 g L^{-1} (GC-R_{40}), 1.51 g L^{-1} (GC-R_{30}), and 0.97g L^{-1} (GC-R_{20}). These values corresponded to an increase of 37.7%, 11.3%, and 9.37%, respectively, compared to P-I.

Production and consumption rate of carboxylic acids in P-II

In P-II, both P_{rate} and C_{rate} of carboxylic acids were relatively higher than P-I. P_{rate} of H_{Ac} was 1.12 (GC-R_{20}), 1.11 (GC-R_{30}) and 2.21 (GC-R_{40}) times higher with gas recirculation strategy compared to non-gas circulated reactors (Fig. 7). While the C_{rate} of H_{Ac} was higher with GC-R_{40} (-0.17 g COD per L per day)
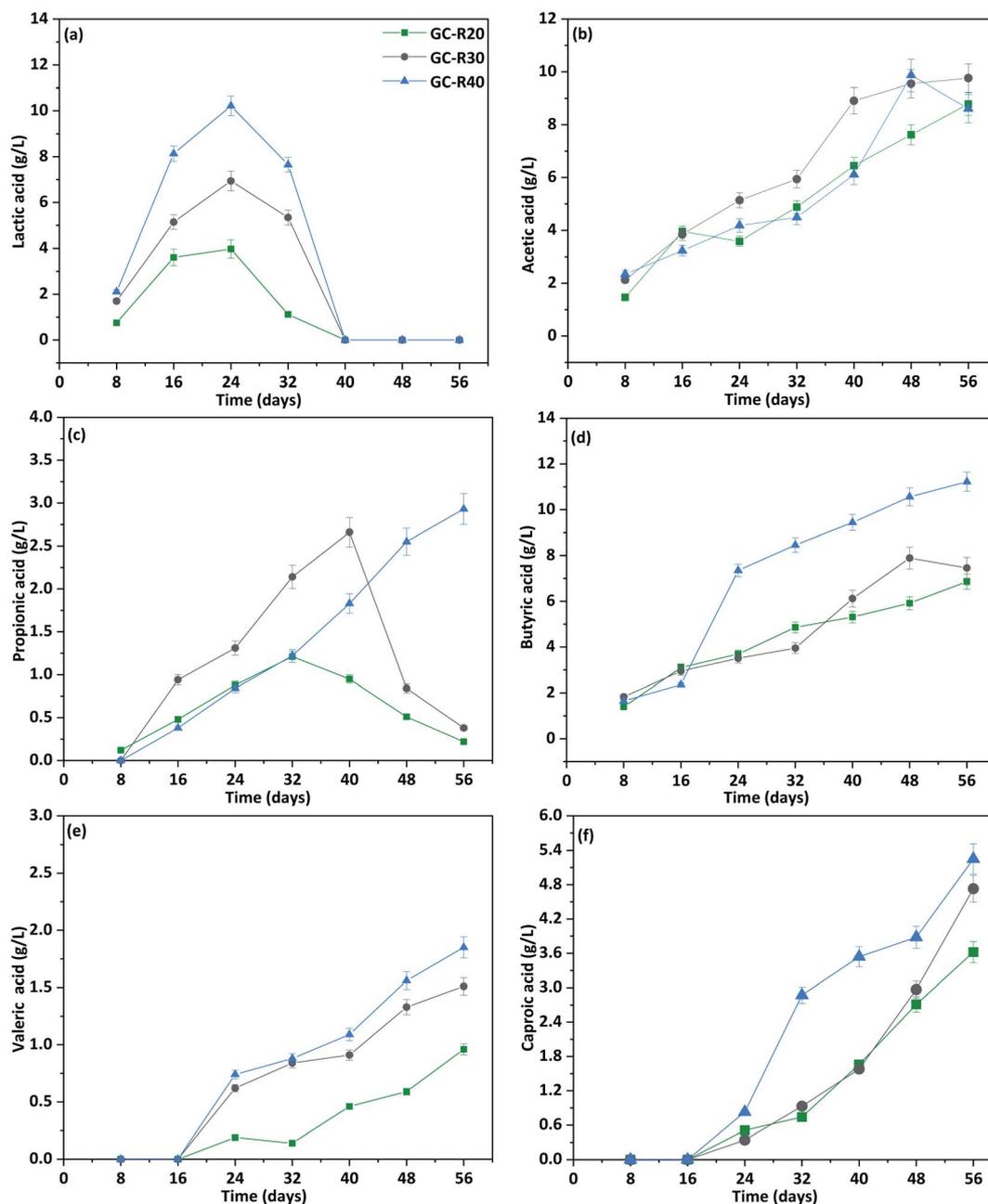
Fig. 6 Influence of biogas recirculation on the composition of carboxylic acids (a–f) observed during P-II operation.

(Fig. 7b). In case of H_{Pr}, its P_{rate} was greater in P-I (0.66–4.75 times higher than P-II), whereas its C_{rate} was 1.1–6.27 times higher specifically with GC-R_{20} and GC-R_{30} in P-II over P-I indicating its possible conversion to H_{Val}. Previous studies reported the concepts and possible routes involved in elongation of H_{Pr} to H_{Val} by chain elongating microbes.[55] On the other side, consumption of H_{Pr} was zero in GC-R_{40} both in P-I and P-II, indicating its continuous production with a P_{rate} ranging between 0.04–0.17 g COD per L per day in the reactor (Fig. 7c). While, the P_{rate} pattern of H_{Bu} between R_{20} and GC-R_{20} was more or less similar until day 40. However, its consumption between days 48–56, (C_{rate}: −0.05 to −0.17 g COD per L per day)

declined its value to 7.48 g COD per L in R_{20}. While an uninterrupted production in GC-R_{20} from day 48 to 56 (P_{rate}: 0.14 to 0.21 g COD per L per day) resulted with net H_{Bu} accumulation of 12.49 g COD per L. The reactors loaded with 30 g COD per L, showed a similar trend of H_{Bu} P_{rate} as observed with 30 g COD per L in P-I. Here the P_{rate} was almost similar with R_{30} and GC-R_{30} till day 40, which further decreased in R_{30} from day 48 (P_{rate}: 0.05–0.23 g COD per L per day) whereas its consumption was noticed with GC-R_{30} on day 56. When the CW load was 40 g COD per L, the maximum H_{Bu} P_{rate} was noticed on day 24 (1.14–1.15 g COD per L per day). Later from day 32 to 48, its P_{rate} ranged between 0.22 to 0.25 g COD per L per day, which increased its

production to 20.42 g COD per L in GC-R$_{40}$. Whereas the final production was limited to 18 g COD per L due to a lower P_{rate} (0.02 to 0.11 g COD per L per day) during the same course of fermentation time in R$_{40}$. An enhanced productivity of H$_{Bu}$ with GC-R$_{20}$, R$_{30}$, R$_{40}$ might be due to direct reduction of CO$_2$ and H$_2$ facilitated through gas recirculation (Fig. 7d). Production of H$_{Val}$ was slightly higher in the reactor loaded 40 g COD per L of CW (R$_{40}$ and GC-R$_{40}$) with a P_{rate} ranging between 0.04-0.19 g COD per L/day followed by 30 g COD per L (R$_{30}$ and GC-R$_{30}$; 0.02–0.16 g COD per L per day) and 20 g COD/L (R$_{20}$ and GC-R$_{20}$; 0.03–0.1 g COD per L per day) (Fig. 7e). The P_{rate} of H$_{Ca}$ was varied in all the reactors at different organic load of CW, which influenced its accumulation. With 20 g COD per L load, the maximum P_{rate} was recorded on day 40 (0.29 g COD per L per day) in GC-R$_{20}$ which was 5.75 times higher over R$_{20}$. Whereas the maximum P_{rate} (0.55 g COD per L per day) with GC-R$_{30}$ was noticed from day 48–56 which was 1.5 times higher than R$_{30}$. The P_{rate} with GC-R$_{40}$ was maximum between day 24–32 (0.26 to 0.63 g COD per L per day) led with accumulation with highest H$_{Ca}$ production (13.02 g COD per L) among all the reactors (Fig. 7f). The P_{rate} was 1.46–2.68 times higher than R$_{40}$. Chain elongated H$_{Ca}$ production through the reverse β-oxidation pathway was significantly higher with function of gas recirculation. This can be attributed the availability of electron either in the form of lactic acid/bioH$_2$ through continuous recirculation as its formation requires electron donor. Additionally CO$_2$ can be reduced to one mole of H$_{Ca}$ which requires 32 electrons while only 8 electrons are needed to convert CO$_2$ to acetate (eqn (4) and (5)).[56]

$$6HCO_3^- + 37H^+ + 32e^- \rightarrow CH_3(CH_2)_4COO^- + 16H_2O \quad (4)$$

$$2HCO_3^- + 9H^+ + 8e^- \rightarrow C_2H_3O_2^- + 4H_2O \quad (5)$$

Chain elongation in phase-I (P-I)

H$_{Ca}$ was detected first on day 24 at 0.56–0.57 g L^{-1} (Fig. 3f), but was almost double by day 40 in all reactors, with the highest value (2.71 g L^{-1}) recorded with R$_{40}$, followed by 1.49 g L^{-1} (R$_{30}$) and 0.84 g L^{-1} (R$_{20}$). H$_{Ca}$ production was accompanied by simultaneous H$_{Lac}$ consumption (Fig. 3a), indicating that the latter was used as an electron donor in the chain elongation process. The highest H$_{Lac}$ production and consumption rates were observed in reactor R$_{40}$ (Fig. 3a). For all reactors, the highest H$_{Lac}$ production rate was observed on day 16 with R$_{40}$ (0.68 g L^{-1} per day), followed by R$_{30}$ (0.33 g L^{-1} per day) and R$_{20}$ (0.31 g L^{-1} per day). Consumption of accumulated H$_{Lac}$ started on day 24, particularly with R$_{20}$ (−0.18 g L^{-1} per day), while production was still positive for R$_{30}$ (0.32 g L^{-1} per day) and R$_{40}$ (0.22 g L^{-1} per day) (). This difference in H$_{Lac}$ conversion between individual reactors highlights the significant role played by the initial concentration of lactose in the medium. Several studies have documented H$_{Ca}$ production from ethanol-containing substrate; however, chain elongation using real field waste/wastewater as substrate requires addition of an external electron donor.[41] In this study, H$_{Lac}$ produced from lactose-containing CW by mixed culture fermentation aided in the formation of H$_{Ca}$. From day 32, the consumption of H$_{Lac}$ increased in all reactors at a rate of −0.56 g L^{-1} per day (R$_{40}$), −0.33 g L^{-1} per day (R$_{30}$), and −0.2 g L^{-1} per day (R$_{20}$). Finally, by day 56, H$_{Lac}$ was fully consumed (). At this point, the highest fraction of H$_{Ca}$ was displayed by R$_{40}$ (4.68 g L^{-1}), followed by R$_{30}$ (3.61 g L^{-1}) and R$_{20}$ (2.66 g L^{-1}) (Fig. 3f).
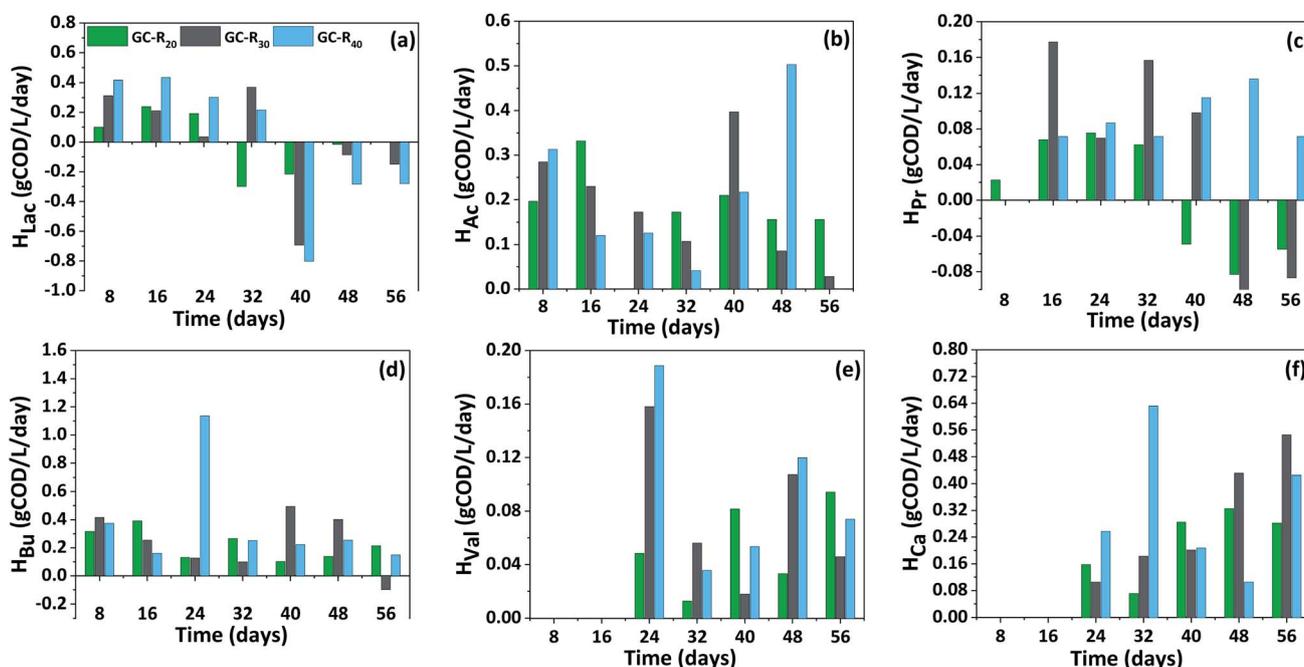

Fig. 7 Distribution of carboxylic acids production (P_{rate}) and consumption rate (C_{rate}) pattern in P-II (a–f) with respect to fermentation time.

Table 2   Acidogenic conversion of BSG loaded with a varied organic load of CW to carboxylic acids in two different phase operation (P-I and P-II)

P-I																	
H_{Lac} (g COD per L)			H_{Ac} (g COD per L)			H_{Pr} (g COD per L)			H_{Bu} (g COD per L)			H_{Val} (g COD per L)			H_{Ca} (g COD per L)		
R_{20}	R_{30}	R_{40}	R_{20}	R_{30}	R_{40}	R_{20}	R_{30}	R_{40}	R_{20}	R_{30}	R_{40}	R_{20}	R_{30}	R_{40}	R_{20}	R_{30}	R_{40}
Day 24	2.68	4.49	8.45	3.85	4.92	4.07	0.6	1.69	0.72	6.22	5.41	12.52	—	—	—	1.39	—	1.41
Day 48	—	1.39	3.32	6.74	8.95	7.92	1.21	1.87	3.4	8.86	10.63	16.82	1.01	1.73	2.33	4.69	6.05	8.7
Day 56	—	—	0.21	8.45	8.97	8.13	0.91	1.72	3.53	7.48	12.45	18.01	1.77	1.92	3.35	6.6	8.95	11.61

Note: In the P-I table the Day rows align across the six acid groups (H_{Lac}, H_{Ac}, H_{Pr}, H_{Bu}, H_{Val}, H_{Ca}) each with R_{20}, R_{30}, R_{40} columns.

P-II (biogas recirculation)																	
H_{Lac} (g COD per L)			H_{Ac} (g COD per L)			H_{Pr} (g COD per L)			H_{Bu} (g COD per L)			H_{Val} (g COD per L)			H_{Ca} (g COD per L)		
GC-R_{20}	GC-R_{30}	GC-R_{40}	GC-R_{20}	GC-R_{30}	GC-R_{40}	GC-R_{20}	GC-R_{30}	GC-R_{40}	GC-R_{20}	GC-R_{30}	GC-R_{40}	GC-R_{20}	GC-R_{30}	GC-R_{40}	GC-R_{20}	GC-R_{30}	GC-R_{40}
Day 24	4.26	4.47	9.21	3.84	5.50	4.47	1.33	1.98	1.27	6.72	6.39	13.38	0.39	1.26	1.51	1.26	0.84	2.06
Day 48	—	1.20	2.25	8.15	10.22	10.56	0.77	1.27	3.85	10.77	14.36	19.22	1.2	2.71	3.18	6.72	7.37	9.62
Day 56	—	—	—	9.41	10.44	9.21	0.33	0.57	4.42	12.49	13.58	20.42	1.96	3.08	3.77	8.98	11.73	13.02

H_{Lac} is thought to act as an electron donor also in the acrylate pathway for the production of H_{Pr}, rather than to generate H_{Ca} via reverse β-oxidation.[41] Such phenomenon was not observed in the present study, as indicated by a rather stable concentration of H_{Pr} throughout the experimental period (Fig. 3c). Besides lactic acid and ethanol, sugars can also donate electrons during microbial chain elongation, leading to H_{Ca} production via two-carbon increments.[15,20,41] Recent studies suggest that H_{Lac} plays an important role in chain elongation of SCCA to MCCA.[20,41] However, mixed culture fermentation of complex substrates results also in other intermediates such as ethanol, making it difficult to determine the exact role of each molecule in chain elongation. Because in this study ethanol production was only 0.3–0.5 g L^{-1}, it likely played only a minor role in the process. Therefore, we believe that MCCA production was achieved mostly through lactic acid utilisation.

Chain elongation during gas recirculation in phase-II (P-II)

The availability of H_{Lac} along with continuous supplementation of an electron donor through gas recirculation in the fermenting medium not only improved accumulation of the SCCA mixture in the reactor, but also enhanced the biosynthesis of H_{Ca}. The concentration of H_{Ca} in P-II reached 5.25 g L^{-1} (GC-R_{40}), followed by 4.73 g L^{-1} (GC-R_{30}) and 3.62 g L^{-1} (GC-R_{20}) (Fig. 6f), which accounted for an increment of 10.85%, 23.67%, and 26.51%, respectively, over P-I (Fig. 3f). This observation was in line with the report by Shuai et al. (2019), who observed better chain elongation from mixed acids compared to pure H_{Ac} due to the beneficial presence of H_{Pr} + H_{Bu} in the fermenting medium.[57] An enhanced H_{Ca} production could be related also to chain elongation in the presence of both H_{Lac} as electron donor and homoacetogenic bacteria as a source of sufficient substrate for the process. Both production and consumption of H_{Lac} were influenced by gas recirculation, with the former being slightly higher than in P-I (Fig. 6a). Maximum production rate of H_{Lac} was achieved by GC-R_{40} (0.75 g L^{-1} per day), followed by GC-R_{30}

(0.43 g L^{-1} per day) and GC-R_{20} (0.35 g L^{-1} per day) on day 16. The consumption rate of H_{Lac} was also greater, particularly with GC-R_{20} (−0.35 g L^{-1} per day) on day 32, followed by GC-R_{40} (−0.95 g L^{-1} per day) and GC-R_{30} (−0.66 g L^{-1} per day) on day 40. This result suggested a key role for lactose-derived H_{Lac} as an intermediate during reverse β-oxidation and consequent chain elongation. The latter was further promoted by the presence of an additional electron donor in the form of bio-H_2 during P-II. Indeed, after complete consumption of H_{Lac}, the recirculating gas in the reactor played an important role in converting CO_2 to metabolites. By day 40, as the accumulated H_{Lac} in the fermenting media was completely utilized, at this point the production of chain elongated carboxylic acids can be attributed to the availability of H_2 in the reactor through its recirculation acting as an electron donor, as the H_2 consumption during this course of time was 2.01 L (GC-R_{30}) followed by 1.9 L (GC-R_{40}) and 1.61 L (GC-R_{20}). At the same time, during reverse β-oxidation, acetate is elongated to butyrate via acetyl-CoA and then butyrate is elongated to caproate via butyl-CoA.[58] Zhang et al. (2013) generated a mixture of carboxylic acids (H_{Ac} + H_{Bu} + H_{Ca}) when fermenting a gas composed of CO_2 (40%) and H_2 (60%) in a hollow-fibre membrane biofilm reactor containing a mixed culture.[59] The COD equivalent of the carboxylic acids produced from co-fermenting BSG and cheese whey wastewater in two different phases is presented in Table 2.

Conclusions

The present study shows that complementing two different waste streams, such as CW and BSG as co-fermenting substrates, increases the output of carboxylic acids and bio-H_2. Lactic acid biosynthesis is dependent on the initial load of CW. A higher load of CW (40 g COD per L) maximised the production of SCCA to 0.38 g L^{-1} per day, which was about 1.2 to 1.6 times higher than using 20 or 30 g COD per L, respectively. Bio-H_2 recovery was maximal with 30 g COD per L. Importantly,

gas recirculation allowed acidogenic CO_2 to be converted to SCCA at a much higher rate (19.9%) compared to the case without gas recirculation. MCCA production, which requires an electron donor, correlated with the consumption of lactic acid, indicating a lactic acid-based chain elongation process. Finally, the enhanced production of MCCA such as caproic acid, after complete utilisation of lactic acid in the fermenting medium, highlights the benefit of gas recirculation as a source of H_2 and its role as a key electron donor.

Author contributions

Omprakash Sarkar: conceptualization, methodology, investigation, writing – original draft; Ulrika Rova: conceptualization, writing – review & editing; Paul Christakopoulos: conceptualization, writing – review & editing; Leonidas Matsakas: conceptualization, methodology, writing – review & editing, supervision.

Conflicts of interest

There are no conflicts to declare.

Acknowledgements

References

1 C. Wang and D. Astruc, *Chem. Soc. Rev.*, 2021, **50**, 3437–3484.
2 E. Zanuso, D. G. Gomes, H. A. Ruiz, J. A. Teixeira and L. Domingues, *Sustainable Energy Fuels*, 2021, **5**, 4233–4247.
3 O. Sarkar, R. Katakojwala and S. Venkata Mohan, *Green Chem.*, 2021, **23**, 561–574.
4 S. Kim, G. Kim and A. Manthiram, *Sustainable Energy Fuels*, 2021, **5**(20), 5024–5037.
5 A. Valente, V. Tulus, Á. Galán-Martín, M. A. J. Huijbregts and G. Guillén-Gosálbez, *Sustainable Energy Fuels*, 2021, **5**(18), 4637–4649.
6 B. Satari, K. Karimi and R. Kumar, *Sustainable Energy Fuels*, 2019, **3**, 11–62.
7 S. Dahiya, S. Chatterjee, O. Sarkar and S. V. Mohan, *Bioresour. Technol.*, 2021, **321**, 124354.
8 M. Ramos-Suarez, Y. Zhang and V. Outram, *Current Perspectives on Acidogenic Fermentation to Produce Volatile Fatty Acids from Waste*, Springer Netherlands, 2021.
9 M. V. Reddy, S. V. Mohan and Y. C. Chang, *Sustainable Energy Fuels*, 2018, **2**, 372–380.
10 S. Dahiya, O. Sarkar, Y. V. V Swamy and S. Venkata Mohan, *Bioresour. Technol.*, 2015, **182**, 103–113.
11 M. V. Reddy and Y.-C. Chang, *Sustainable Energy Fuels*, 2021, **5**, 4133–4140.
12 L. T. Angenent, H. Richter, W. Buckel, C. M. Spirito, K. J. J. J. Steinbusch, C. M. Plugge, D. P. B. T. B. B. T. B. Strik, T. I. M. M. Grootscholten, C. J. N. N. Buisman and H. V. M. M. Hamelers, *Environ. Sci. Technol.*, 2016, **50**, 2796–2810.
13 L. A. Kucek, C. M. Spirito and L. T. Angenent, *Energy Environ. Sci.*, 2016, **9**, 3482–3494.
14 O. Sarkar, U. Rova, P. Christakopoulos and L. Matsakas, *J. Environ. Chem. Eng.*, 2021, **9**, 105990.
15 K. J. J. J. Steinbusch, H. V. M. M. Hamelers, C. M. Plugge and C. J. N. N. Buisman, *Energy Environ. Sci.*, 2011, **4**, 216–224.
16 C. M. Spirito, H. Richter, K. Rabaey, A. J. M. M. Stams and L. T. Angenent, *Curr. Opin. Biotechnol.*, 2014, **27**, 115–122.
17 M. T. Agler, B. A. Wrenn, S. H. Zinder and L. T. Angenent, *Trends Biotechnol.*, 2011, **29**, 70–78.
18 Q. Wang, P. Zhang, S. Bao, J. Liang, Y. Wu, N. Chen, S. Wang and Y. Cai, *Bioresour. Technol.*, 2020, **306**, 123188.
19 W. d A. Cavalcante, R. C. Leitão, T. A. Gehring, L. T. Angenent and S. T. Santaella, *Process Biochem.*, 2017, **54**, 106–119.
20 P. Candry, L. Radić, J. Favere, J. M. Carvajal-Arroyo, K. Rabaey and R. Ganigué, *Water Res.*, 2020, **186**, 116396.
21 H. B. Ding, G. Y. A. Tan and J. Y. Wang, *Bioresour. Technol.*, 2010, **101**, 9550–9559.
22 M. T. Agler, C. M. Spirito, J. G. Usack, J. J. Werner and L. T. Angenent, *Energy Environ. Sci.*, 2012, **5**, 8189–8192.
23 A. Duber, L. Jaroszynski, R. Zagrodnik, J. Chwialkowska, W. Juzwa, S. Ciesielski and P. Oleskowicz-Popiel, *Green Chem.*, 2018, **20**, 3790–3803.
24 D. Vasudevan, H. Richter and L. T. Angenent, *Bioresour. Technol.*, 2014, **151**, 378–382.
25 R. Karki, W. Chuenchart, K. C. Surendra, S. Shrestha, L. Raskin, S. Sung, A. Hashimoto and S. Kumar Khanal, *Bioresour. Technol.*, 2021, **330**, 125001.
26 M. R. Al Mamun, S. Torii, M. M. Rahman and M. R. Karim, *Sustainable Energy Fuels*, 2019, **3**, 166–172.
27 K. Amulya and S. Venkata Mohan, *Chem. Eng. J.*, 2022, **429**, 132163.
28 S. Schlager, A. Fuchsbauer, M. Haberbauer, H. Neugebauer and N. S. Sariciftci, *J. Mater. Chem. A*, 2017, **5**, 2429–2443.
29 D. Li, H. Zhang, H. Xiang, S. Rasul, J.-M. Fontmorin, P. Izadi, A. Roldan, R. Taylor, Y. Feng, L. Banerji, A. Cowan, E. H. Yu and J. Xuan, *Sustainable Energy Fuels*, 2021, **5**, 5893–5914.
30 H. Ostovari, A. Sternberg and A. Bardow, *Sustainable Energy Fuels*, 2020, **4**, 4482–4496.
31 G. Mohanakrishna, J. S. Seelam, K. Vanbroekhoven and D. Pant, *Faraday Discuss.*, 2015, **183**, 445–462.
32 M. Alfano and C. Cavazza, *Sustainable Energy Fuels*, 2018, **2**, 1653–1670.
33 J. Annie Modestra, R. Katakojwala and S. Venkata Mohan, *Chem. Eng. J.*, 2020, **394**, 124759.

34 S. Bolognesi, L. Bañeras, E. Perona-Vico, A. G. Capodaglio, M. D. Balaguer and S. Puig, *Sustainable Energy Fuels*, 2022, **6**(1), 150–161.

35 L. Matsakas, O. Sarkar, S. Jansson, U. Rova and P. Christakopoulos, *Bioresour. Technol.*, 2020, **316**, 123973.

36 O. Sarkar, U. Rova, P. Christakopoulos and L. Matsakas, *Bioresour. Technol.*, 2021, **319**, 124233.

37 M. Ribau Teixeira, E. C. Guarda, E. B. Freitas, C. F. Galinha, A. F. Duque and M. A. M. Reis, *New Biotechnol.*, 2020, **57**, 4–10.

38 S. Liang and C. Wan, *Bioresour. Technol.*, 2015, **182**, 179–183.

39 E. C. Guarda, A. C. Oliveira, S. Antunes, F. Freitas, P. M. L. Castro, A. F. Duque and M. A. M. Reis, *Appl. Sci.*, 2021, 11.

40 S. I. Mussatto, M. Fernandes, G. Dragone, I. M. Mancilha and I. C. Roberto, *Biotechnol. Lett.*, 2007, **29**, 1973–1976.

41 J. Xu, J. Hao, J. J. L. Guzman, C. M. Spirito, L. A. Harroff and L. T. Angenent, *Joule*, 2018, **2**, 280–295.

42 K. V Venkatesh, M. R. Okos and P. C. Wankat, *Process Biochem.*, 1993, **28**, 231–241.

43 H.-Q. Yu, Y. Mu and H. H. P. Fang, *Biotechnol. Bioeng.*, 2004, **87**, 813–822.

44 B. Lagoa-Costa, C. Kennes and M. C. Veiga, *Bioresour. Technol.*, 2020, **308**, 123226.

45 M. Atasoy, O. Eyice and Z. Cetecioglu, *Bioresour. Technol.*, 2020, **311**, 123529.

46 R. A. Gonzalez-Garcia, T. McCubbin, L. Navone, C. Stowers, L. K. Nielsen and E. Marcellin, *Fermentation*, 2017, **3**, 1–20.

47 R. Rao and N. Basak, *Appl. Biochem. Biotechnol.*, 2021, **193**(7), 2297–2330.

48 S. Venkata Mohan, G. N. Nikhil, P. Chiranjeevi, C. Nagendranatha Reddy, M. V. Rohit, A. N. Kumar and O. Sarkar, *Bioresour. Technol.*, 2016, **215**, 2–12.

49 J. Rajesh Banu, G. Ginni, S. Kavitha, R. Yukesh Kannah, S. Adish Kumar, S. K. Bhatia and G. Kumar, *Bioresour. Technol.*, 2021, **319**, 124241.

50 P. Dessì, F. Asunis, H. Ravishankar, F. G. Cocco, G. De Gioannis, A. Muntoni and P. N. L. Lens, *Int. J. Hydrogen Energy*, 2020, **45**, 24453–24466.

51 A. Schievano, A. Tenca, B. Scaglia, G. Merlino, A. Rizzi, D. Daffonchio, R. Oberti and F. Adani, *Environ. Sci. Technol.*, 2012, **46**, 8502–8510.

52 G. Luo, D. Karakashev, L. Xie, Q. Zhou and I. Angelidaki, *Biotechnol. Bioeng.*, 2011, **108**, 1816–1827.

53 D. Arslan, K. J. J. Steinbusch, L. Diels, H. De Wever, C. J. N. Buisman and H. V. M. Hamelers, *Bioresour. Technol.*, 2012, **118**, 227–234.

54 M. Zhou, J. Zhou, M. Tan, J. Du, B. Yan, J. W. C. Wong and Y. Zhang, *Bioresour. Technol.*, 2017, **245**, 44–51.

55 H. Kim, B. S. Jeon and B.-I. Sang, *Sci. Rep.*, 2019, **9**, 11999.

56 R. Lin, C. Deng, W. Zhang, F. Hollmann and J. D. Murphy, *Trends Biotechnol.*, 2021, **39**, 370–380.

57 B. Shuai, Z. GuangMing, Z. PanYue, W. QingYan, Z. YaZhou, T. Xue, W. SiQi, N. Mohammad, C. YaJing and F. Wei, *Int. J. Agric. Biol.*, 2019, **22**, 1613–1622.

58 X. Chen and B.-J. Ni, *Chem. Eng. J.*, 2016, **306**, 1092–1098.

59 F. Zhang, J. Ding, N. Shen, Y. Zhang, Z. Ding, K. Dai and R. J. Zeng, *Appl. Microbiol. Biotechnol.*, 2013, **97**, 10233–10240.